Single Crystal Trigonal Selenium Nanoplates Converted from Selenium Nanoparticles

Haoyong Yin, Zhude Xu,* Huahui Bao, Jingyi Bai, and Yifan Zheng
*Chemistry Department of Zhejiang University, Hangzhou, 310027, P. R. China*

The single crystal trigonal selenium nanoplates have been prepared directly from the trigonal selenium nanoparticles in a simple way with ethylenediamine in existence. The as-prepared nanoplates were characterized by XRD, TEM, HRTEM, SEM, and SAED measurements. It is shown that the selenium nanoplates have a single crystalline structure with the length and width reaching up to several microns while their thickness being only about 50 nm. This preparation method may be extended to the fabrication of other 2D elemental crystals with the similar crystal structures of trigonal selenium.

Recently, great efforts have been made to synthesize one-dimensional (1D)[1] and two-dimensional (2D)[2] nanostructures because of their unique optoelectronic, magnetic, and mechanical properties, as well as their applications in the mesoscopic research and nanodevices.[3] In the previous research works the synthesis of 1D single crystal trigonal selenium (t-Se) nanowires have attracted great interests for their excellent physical and chemical properties.[4–8] Trigonal selenium is a p-type extrinsic semiconductor with an indirect bandgap of about 1.6 eV. It has been widely used in producing photocells, photographic exposure meters, pressure sensors, and electrical rectifiers because of its high photoconductivity, excellent spectral sensitivity, and large piezoelectric, thermoelectric, and nonlinear responses.[9] Moreover, it is well known that the t-Se nanowires and nanorods could be directly nucleated and grown from their aqueous solution without using any physical templates owing to their crystal structures consisting of extended and helical chains. On the basis of this knowledge, Xia's group and other groups have successfully fabricated rod-like or wire-like 1D single crystal selenium materials by different methods.[4–9] However, to the best of our knowledge, there have been no reports yet on the preparation of 2D nanoplates of t-Se.

In this letter, we report the ethylenediamine-assisted growth of 2D single crystal t-Se nanoplates via the hydrothermal procedure. During the experimental process, the t-Se nanoparticles were preferentially converted into 2D t-Se nanoplates in the reaction solution. This solid–solution–solid (SSS) process may be different from the previous vapor–solid (VS) process[5,6] or sonochemical process[8] in the preparation of 1D nanowires. Acordingly, the growing mechanism of the single crystal 2D structures may also differ from that of 1D structures. In addition, Se can react readily with other elements to generate a wealth of functional materials. For example, $RuSe_2$ and $Pd_{17}Se_{15}$ nanotubes can be synthesized by reacting precursor salts with selenium nanowires.[10] The availability of 2D Se nanostructures will be able to bring in new types of applications or to enhance the performance of the current devices as a result of size confinement. In the present experiment, 1.0-g t-Se was suspended in 30-mL water through supersonic treatment, then 10-mL ethylenediamine was mixed with the solution uniformly. After that, the mixed so-

lution was transferred to a Teflon-lined autoclave which was then sealed into a stainless-steel tank and heated at 150 °C for 24 h. After cooling down to room temperature, a black precipitate was collected, washed with water several times, and dried in air at 60 °C. Through such a SSS process, the nanoplate product was finally produced.
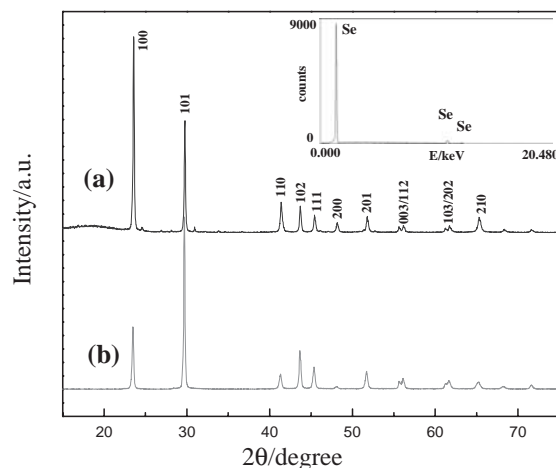
Figure 1. The XRD patterns of the t-Se nanoplates (a) and the stock t-Se nanoparticles (b). The insert is the EDX pattern of the t-Se nanoplates.

The crystallinity and purity (composition and phase) of the as-prepared nanoplates were characterized with X-ray powder diffraction (XRD, X'pert MPD Philips X-ray diffractometer) and energy dispersive X-ray (EDX) measurements. Figure 1 shows the typical XRD patterns of the product nanoplates and the stock t-Se nanoparticles (the insert is the EDX pattern of the nanoplates). It can be observed that the nanoplates have the same diffraction peaks with the stock t-Se nanoparticles. The strong and sharp diffraction peaks of the two samples were indexed to the trigonal phase of selenium. The XRD pattern of the nanoplates suggests that it has a high crystallinity. The calculated lattice constants of $a = 4.362$ and $c = 4.958$ Å are consistent with the literature data of $a = 4.366$ and $c = 4.955$ Å (JCPDS file, No. 6-362). The abnormal intensity of the (100) peak and the distinct appearance of the (200) peak (as compared to that of the stock t-Se nanoparticles) indicate that these selenium nanoplates have been preferentially grown along the c axis and a axis, the [001] direction and the [100] direction. The EDX pattern shows that the nanoplates are pure selenium.

The morphology and structure of the nanoplates were also characterized by transmission electron microscopy (TEM, JEM-200CX), high-resolution TEM (HRTEM) and selected-area electron diffraction (SAED). Figures 2a and 2b show the TEM images of the stock t-Se nanoparticles and the t-Se nano-
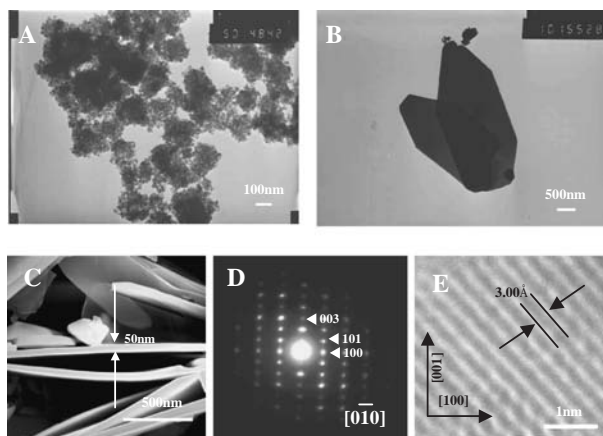
Figure 2. A) TEM image of the stock t-Se nanoparticles. B) TEM image of the t-Se nanoplates. C) SEM image of the nanoplates. D) SAED pattern of the nanoplates. E) HRTEM image of the nanoplates.

plates. It can be seen that the stock materials are composed of uniform nanoparticles with diameters less than 20 nm. The TEM image of the nanoplates reveals that they have good crystallinity and uniformity but a much lower aspect ratio than that of the nanowires or nanobelts reported in the literature.[4-9] The length and width of the nanaoplates can reach up to several microns in dimension, while the thickness is about 50 nm in average as shown in the scanning electron microscopy image (SEM, AMRAY 1840) (Figure 2c). In Figure 2b, two distinct side edges can be clearly observed at the tip of the single crystal nanoplates. It suggests that the nanoplates may grow along two different directions. Figure 2d shows a typical SAED pattern of the nanoplates which was obtained by focusing the electron beam to the plane surface of the nanoplates. Through careful analysis of this diffraction pattern, the diffraction spots can be distinguished and indexed as marked in the figure. Also, the $[0\bar{1}0]$ zone axis of the t-Se nanoplates was assigned to perpendicular to the plate plane. These results indicate that the plane surface of the nanoplates corresponds to the $(0\bar{1}0)$ crystallographic planes while the two side edges at the tip may extend along the [100] and [001] crystallographic axis directions, respectively. This may suggest that these t-Se nanoplates had predominantly grown along the [001] and [100] directions, being consistent with the above XRD study results. The lattice constants ($a = 4.322$ and $c = 4.934$ Å) calculated from this diffraction pattern also agree well with those of the trigonal phase reported in literature. When focusing the electron beam to the different regions of the individual nanoplate, the same diffraction pattern was obtained. It is concluded that the nanoplates synthesized using the present procedure are single crystalline in structure. This conclusion is also supported by high-resolution TEM (HRTEM) studies (shown in Figure 2e). The clearly observed lattice fringes reveal that the t-Se nanoplates are highly crystalline. The interplanar spacing of 3.00 Å matches well with the space between the (101) lattice planes. Combining the electron diffraction (ED) pattern with the unique structure and internal angles of trigonal selenium, it further leads to the conclusion that the 2D t-Se nanoplates grow along the [001] and [100] directions.

The process of the ethylenediamine-assisted growth of t-Se nanoplates may be described as follows. At the first step, the t-Se nanoparticles were partially dissolved into the reaction solution during the hydrothermal treatments. After saturation, with the assistance of the ethylenediamine, the saturated t-Se solute preferentially crystallized into 2D nanoplates. In t-Se nanoparticles dissolving, obviously the reverse process, namely the dissolved t-Se precipitates into t-Se particles, could also occur. Nevertheless, it seemed that the dissolved t-Se prefers to grow into 2D nanoplates in our experimental conditions. There might be several reasons such as a) the trigonal crystal structure of the t-Se makes it in favor of growing along certain axes. b) the surface area of the t-Se nanoparticles is much larger than the nanoplates so that the nanoplates with less surface energy are more thermodynamically stable. However, the most critical reason is probably the effect of ethylenediamine. When the t-Se nanoparticles were hydrothermally treated in the same procedure but without the addition of ethylenediamine, there were not any changes in the morphology between the stock materials and the products. In addition, the ethylenediamine concentration and reaction temperature also strongly affected the product morphology. The detailed effects of ethylenediamine will be studied in the further investigation.

In summery, we have demonstrated a simple method to synthesize the single crystal t-Se nanoplates with the length and width being several microns in dimension and about 50 nm in thickness. The growth of the nanoplates may be along the *a* and *c* axis which differ from the growth of t-Se nanowires. The 2D t-Se nanoplates may be employed as the template to prepare other kinds of inorganic 2D nanostructures. Besides, this method may also be helpful in the synthesis of other 2D elemental crystals with the similar crystal structures of t-Se.

References
1 Y. Xia, P. Yang, Y. Sun, Y. Wu, B. Mayers, B. Gates, Y. Yin, F. Kim, and H. Yan, *Adv. Mater.*, **15**, 353 (2003).
2 T. S. Ahmadi, Z. L. Wang, T. C. Green, A. Henglein, and M. A. Elsayed, *Science*, **272**, 1924 (1996).
3 J. Kim, S. Cha, K. Shin, J. Jho, and J. Lee, *Adv. Mater.*, **16**, 459 (2004).
4 B. Gates, Y. Yin, and Y. Xia, *J. Am. Chem. Soc.*, **122**, 12582 (2000).
5 L. Ren, H. Zhang, P. Tan, Y. Chen, and Z. Zhang, *J. Phys. Chem. B*, **108**, 4627 (2004).
6 X. Cao, Y. Xie, and L. Li, *Adv. Mater.*, **15**, 1914 (2003).
7 X. Liu, M. Mo, J. Zeng, and Y. Qian, *J. Cryst. Growth*, **259**, 144 (2003).
8 B. Mayers, K. Liu, D. Sunderland, and Y. Xia, *Chem. Mater.*, **15**, 3852 (2003).
9 X. Cao, Y. Xie, S. Zhang, and F. Li, *Adv. Mater.*, **16**, 649 (2004).
10 X. Jiang, B. Mayers, Y. Wang, B. Cattle, and Y. Xia, *Chem. Phys. Lett.*, **385**, 472 (2004).